Environ. Sci. Technol. **2006**, *40,* 3912−3921

Single Particle Characterization of Ultrafine and Accumulation Mode Particles from Heavy Duty Diesel Vehicles Using Aerosol Time-of-Flight Mass Spectrometry

STEPHEN M. TONER, DAVID A. SODEMAN, AND KIMBERLY A. PRATHER*

Department of Chemistry and Biochemistry, Scripps Institution of Oceanography, University of California, San Diego, La Jolla, California 92093-0314

The aerodynamic size and chemical composition of individual ultrafine and accumulation mode particle emissions (D_a = 50−300 nm) were characterized to determine mass spectral signatures for heavy duty diesel vehicle (HDDV) emissions that can be used for atmospheric source apportionment. As part of this study, six in-use HDDVs were operated on a chassis dynamometer using the heavy heavy-duty diesel truck (HHDDT) five-cycle driving schedule under different simulated weight loads. The exhaust emissions were passed through a dilution/residence system to simulate atmospheric dilution conditions, after which an ultrafine aerosol time-of-flight mass spectrometer (UF-ATOFMS) was used to sample and characterize the HDDV exhaust particles in real-time. This represents the first study where refractory species including elemental carbon and metals are characterized directly in HDDV emissions using on-line mass spectrometry. The top three particle classes observed with the UF-ATOFMS comprise 91% of the total particles sampled and show signatures indicative of a combination of elemental carbon (EC) and engine lubricating oil. In addition to the vehicle make/year, the effects of driving cycle and simulated weight load on exhaust particle size and composition were investigated.

Introduction

Of the various anthropogenic sources of particles, diesel powered vehicles have become an increasing environmental concern. While they tend to have lower fuel consumption and CO_2 emissions, on a per vehicle basis, they produce 1−2 orders of magnitude more particulate matter emissions than do gasoline powered vehicles (*1*). Many studies have been conducted on the particulate matter released in diesel emissions. These studies have included insight into the possible health effects (*2*−*5*) as well as size and number concentrations of particles emitted by diesel vehicles (*6*−*16*). Many of these studies have shown that the emissions from diesel engines produce high number concentrations of ultrafine particles, especially during idle and low RPM engine operating conditions. Certain studies have probed the composition of diesel particulate matter using filter and/or impactor techniques, such as micro orifice uniform deposit impactors (MOUDI), to collect particles in different size ranges. Analysis of the particles collected on filters can be useful for determining organic species and the mass of different species; however, no information is acquired on single particle chemistry or rapid changes in chemical composition. Detailed information on the individual particle types emitted by diesel engines is crucial for understanding their origin as well as the type and level of environmental and health impacts they may have. With such a large fraction of particles emitted from diesel vehicles formed in the accumulation and ultrafine size ranges, it is important to be able to accurately apportion these particles, and single particle analysis provides a potentially more direct approach for doing this.

Single particle mass spectrometry techniques, such as aerosol time-of-flight mass spectrometry (ATOFMS), have been used in a number of studies for characterizing particles in the fine (100−1000 nm) and coarse (>1000 nm) size ranges. Recently, the ATOFMS instrument incorporated an aerodynamic lens for improved transmission of smaller accumulation mode and ultrafine particles and is referred to as an ultrafine aerosol time-of-flight mass spectrometer (UF-ATOFMS) (*17*). In this study, the UF-ATOFMS was used to characterize individual ultrafine and accumulation mode diesel exhaust particles. Other particle mass spectrometers, such as the thermal desorption particle beam mass spectrometer (TDPBMS) (*18*−*20*) and the Aerodyne aerosol mass spectrometer (AMS) (*21*, *22*), have been used to characterize particles emitted from diesel engines. The TDPBMS and AMS have been shown to be useful in distinguishing organic carbon particles; however, these techniques cannot measure refractory components in particles, such as elemental carbon, which can represent a significant fraction of diesel emissions particularly in the 50−100 nm size range (*6*, *23*).

The goal of this study is to chemically characterize ultrafine and accumulation mode (50−300 nm, D_a) diesel exhaust particles to determine single particle mass spectral signatures that are unique to heavy duty diesel vehicles (HDDVs). These signatures will be grouped with those obtained from previous ATOFMS studies for HDDV exhaust (100−3000 nm, D_a) and gasoline vehicle (LDV) exhaust (50−3000 nm, D_a) to perform ambient source apportionment of HDDV and LDV exhaust particles. Finally, to examine whether the acquired dynamometer signatures are representative of particles sampled in ambient air, an initial comparison is presented of the acquired HDDV signatures with those obtained during a recent freeway-side ATOFMS study.

Experimental Procedures

Six HDDVs were analyzed in July and August 2003 at the Ralph's Distribution Center in Riverside, CA. A description of each truck is provided in Table 1, including the vehicle/engine year, manufacturer, engine power, miles driven, and driving cycles performed. The HDDVs were tested under the same sampling conditions, including the driving schedule and dilution conditions, so the major aerosol chemical disparities observed between trucks can be attributed to the differences between trucks and not sampling and/or instrumental variability (*24*).

The sampling conditions consisted of driving each truck on a heavy duty dynamometer operated by West Virginia University personnel. The transportable heavy duty vehicle emissions testing laboratory (THDVETL) was used to obtain reproducible aerosol emissions from HDDV and is described elsewhere (*25*, *26*). For this study, the heavy heavy-duty diesel truck (HHDDT) five-cycle driving schedule under different

* Corresponding author phone: (858)822-5312; fax: (858)534-7042; e-mail: kprather@ucsd.edu.

10.1021/es051455x CCC: $33.50
Published on Web 05/18/2006

TABLE 1. Heavy Duty Diesel Vehicles (HDDVs) Tested and Driving Cycles Performed

E55CRC (truck)	Vehicle Model Year	Vehicle Manufacturer	Engine Model Year	Engine Manufacturer	Engine Model	Engine Power (hp)	Mileage	Tests Performed
E55CRC-27	2000	Freightliner	1999	Detroit	Diesel Series 60	500	420,927	C*
E55CRC-28	1999	Freightliner	1998	Detroit	Diesel Series 60	500	539,835	IC, A*
E55CRC-30	1999	Freightliner	1998	Detroit	Diesel Series 60	500	138,553	IC, A
E55CRC-31	1998	Kenworth	1997	Cummins	N14-460E+	460	587,265	A, B
E55CRC-32	1992	Volvo	1991	Caterpillar	3406B	280	595,258	A
E55CRC-33	1985	Freightliner	1984	Caterpillar	3,406	310	988,823	A

Five cycle test at A) 56,000 lbs / B) 66,000 lbs / C) 75,000 lbs

30 min idle
10 min soak
17 min creep
10 min soak
11 min transit
10 min soak
34 min cruise with speeds at 55 mph
10 min soak
13 min "high speed" HDDT_S cycle at 65 mph *(31 min "high speed" HHDDT65 at 65 mph)
stop cycle

56,000 lbs idle-creep cycle (IC)

Idle truck for 30 min
run at "creep" speeds for 17 min
10 min soak with engine off
repeat 5x

simulated on-axle weight loads was used to determine the effect of driving conditions on the exhaust particle's chemical composition. The HHDDT five-cycle schedule was developed by the California Air Resources Board (CARB) and consisted of an idle, creep, transient, cruise, and high-speed cycle.

For this study, an ultrafine aerosol time-of-flight mass spectrometer (UF-ATOFMS) was used to size and chemically characterize HDDV exhaust particles between 50 and 300 nm. The UF-ATOFMS instrument along with a scanning mobility particle sizer (SMPS) (TSI Model 3936L10) sampled off of a stack dilution tunnel (SDT) residence chamber continuously for each truck testing period. Stainless steel sampling lines were used to sample from the residence chamber to the instrumentation and were coupled to the instruments with black conductive tubing (TSI). A more detailed description of the driving cycles and the sampling conditions is provided in the Supporting Information. A diagram of the sampling system is also provided in the Supporting Information, Figure S1 (*27*).

Data obtained from this study were imported into Matlab 6.1.0.450 (Release 12.1) and analyzed with the ART-2a neural network data analysis algorithm (*28*−*30*) using a vigilance factor of 0.85, learning rate of 0.05, and 20 iterations. This method of analysis has been shown to be reliable for ATOFMS data and is used for this study to allow comparisons to be made to previous and future studies using the same technique. Single particle HDDV emissions (100−3000 nm) have been sampled and reported with a standard-inlet ATOFMS instrument previously (*31*) and will be used as a basis of comparison in this paper.

Description of Particle Types Observed with UF-ATOFMS. Formation studies of diesel exhaust particles in the accumulation and ultrafine size mode have been studied and described elsewhere (*1*, *18*, *32*). These previous accounts of HDDV exhaust have mainly focused on size profiles of the exhaust particles or chemical composition obtained using bulk analysis methods. In addition, studies using thermal desorption mass spectrometry for on-line chemical composition analysis have focused on the nonrefractory materials, and thus, the associations between elemental carbon and other species such as metals have not been probed (*18*, *20*, *22*). This study is unique in reporting the results from single particle analysis of the full range of chemical species in ultrafine and accumulation mode particles sampled directly from HDDV. Representative spectra/weight matrices for the seven classes are shown in Figure 1 (A−G), and Figure 2 shows the statistical breakdown of these classes by percentage. It is important to note that these seven classes serve as simplified representations of the particle types to illustrate the major signatures observed and their relative abundances. The method by which the spectra were classified into these seven types is fully described in the Supporting Information. The representative spectra in Figure 1 are shown in order of particle class abundance. This section provides a summary of the particle types detected, while a more detailed description of each class is provided in the Supporting Information.

The top particle class (Figure 1A and labeled EC, Ca, OC, and phosphate in Figure 2) made up 78% of the particles sampled by UF-ATOFMS in the ultrafine and accumulation particle modes. On the basis of the spectrum, the EC particles in this class show primarily short chain carbon envelopes (C_n^+ where $n < 6$). Another note regarding the EC peaks in this class is that the peak for $^{36}C_3^+$ is larger than that for $^{12}C_1^+$. This finding is reproducible for ultrafine HDDV particles and will be addressed later in the discussion of the prospects for ambient apportionment. The calcium and phosphate in this class most likely come from additives typically used in diesel engine lubrication oil (*33*−*35*). These findings suggest that this main class of particles seen in HDDV exhaust can be attributed to engine lubricating oil and/or coagulation of lubricating oil and EC particles from incomplete combustion. These results agree with the findings by other researchers that lubricating oil is detected in the majority of diesel exhaust particles (*18*, *20*, *22*, *36*−*39*).

The second most abundant particle type is shown in Figure 1B (labeled OC, EC, phosphate, and sulfate in Figure 2) and makes up 8% of the particles characterized with the UF-ATOFMS. Given that HDDVs produce a higher fraction of EC as compared to OC (*40*, *41*), it is somewhat surprising that there is an OC particle type that does not contain an EC core. However, it should be noted that while all HDDVs produced this particle type, most of the particles in this OC class came from one HDDV (E55CRC-30). Given the large surface area of EC particles produced in diesel emissions, it is likely that this particle type was produced by large amounts of OC species condensing on EC particle cores.

The third most abundant particle type observed makes up 7% of the HDDV exhaust particles classified with UF-ATOFMS and is represented in Figure 1C (labeled Ca, Na, EC, phosphate, and sulfate in Figure 2). The spectra suggest

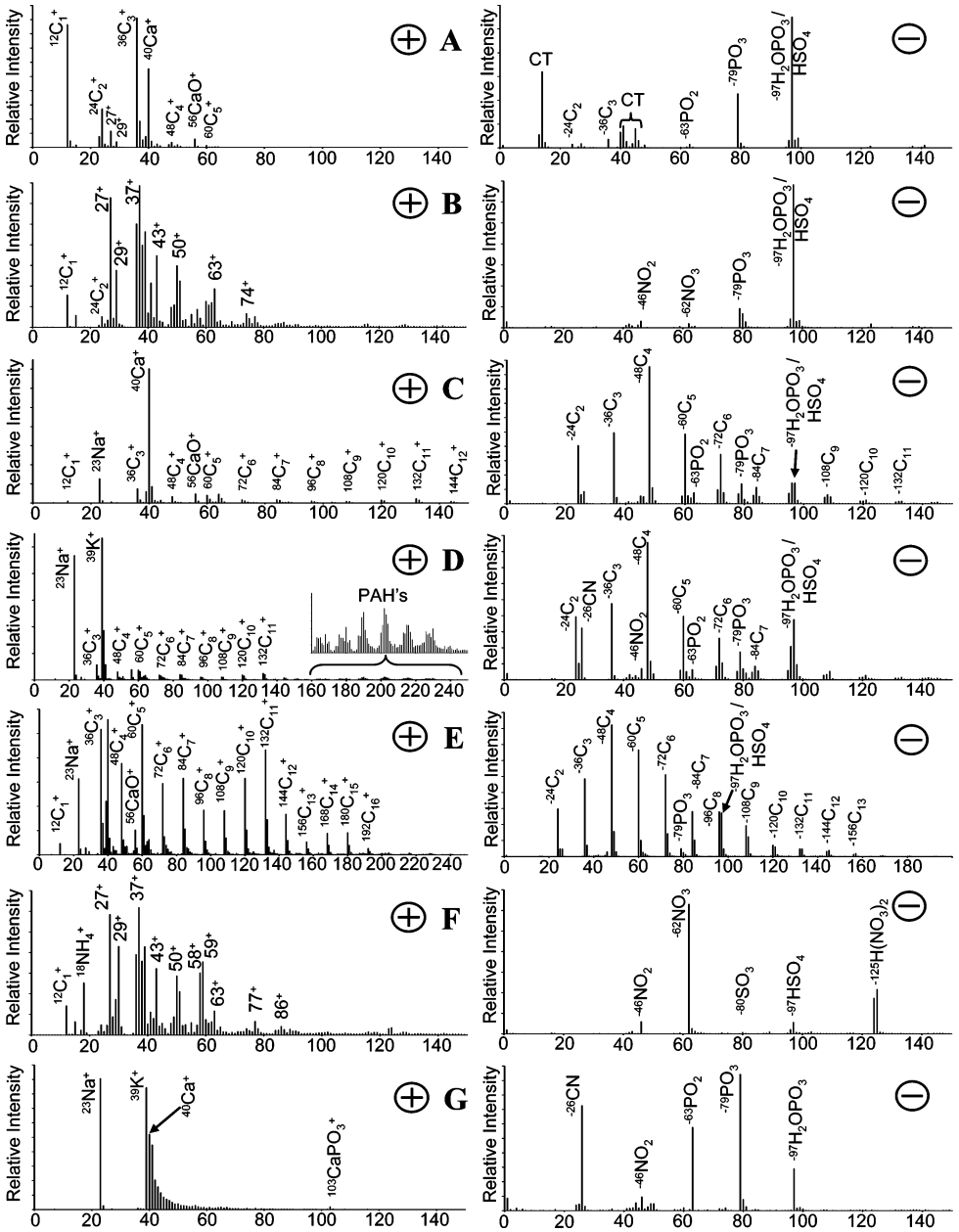

FIGURE 1. (A−G) Positive and negative ion representative mass spectra/weight matrices for the particle classes sampled in HDDV exhaust. Peaks labeled CT in the negative ion spectra indicate signal cross-talk, or noise, from the positive ion detector.

the particles contained lubricating oil as they are very similar to the top class, except that the spectra in this class contain sodium and higher m/z EC fragments. Sodium can come from a variety of sources, including impurities in the lubricating oil and/or from the diesel fuel. Diesel fuel samples analyzed in the lab with an ATOFMS show the presence of sodium more frequently than in the oil samples (*42*). The most reasonable explanations for the higher m/z carbon ion fragments are that the EC peaks in this particle type are produced by larger soot agglomerates or differences in the laser desorption/ionization (LDI) process. It is known that soot can form long-chain EC/soot agglomerates, which grow to their largest sizes in the accumulation mode (*1*, *6*, *43*−*45*). One cannot exclude the possibility that these particles experienced different powers during the LDI process. It has been shown that there are differences with ATOFMS spectra for the same particle type based solely on the LDI laser (*46*). As shown in Wenzel et al., these effects result from ionizing the particle in cold or hot spots of an inhomogeneous laser beam where the power density is different enough to cause softer or harder ionization, respectively. The techniques used by Wenzel et al. for LDI beam homogenization were not used for this study.

The fourth most abundant classified particle type makes up 3% of the total particles and is represented in Figure 1D (labeled as Na, K, Ca, EC, PAH, phosphate, nitrate, and sulfate in Figure 2). Particles in this class appear to contain a mixture of diesel oil and fuel combustion byproducts. The presence of sodium and potassium with such a strong intensity resembles the spectra seen in the lab-analyzed diesel fuel samples (*42*). The presence of PAHs has been seen in both fuel and oil samples and could be from either source or could have formed during combustion and condensed onto the particles. The ATOFMS lab-analyzed fuel samples from Spencer et al. showed much more PAH content in diesel fuel than in gasoline fuel, which is consistent with previous literature findings (*47*, *48*).

The fifth most abundant class, making up 2% of the total HDDV exhaust particles, is represented in Figure 1E (labeled EC, Ca, Na, OC, phosphate, and sulfate in Figure 2). While

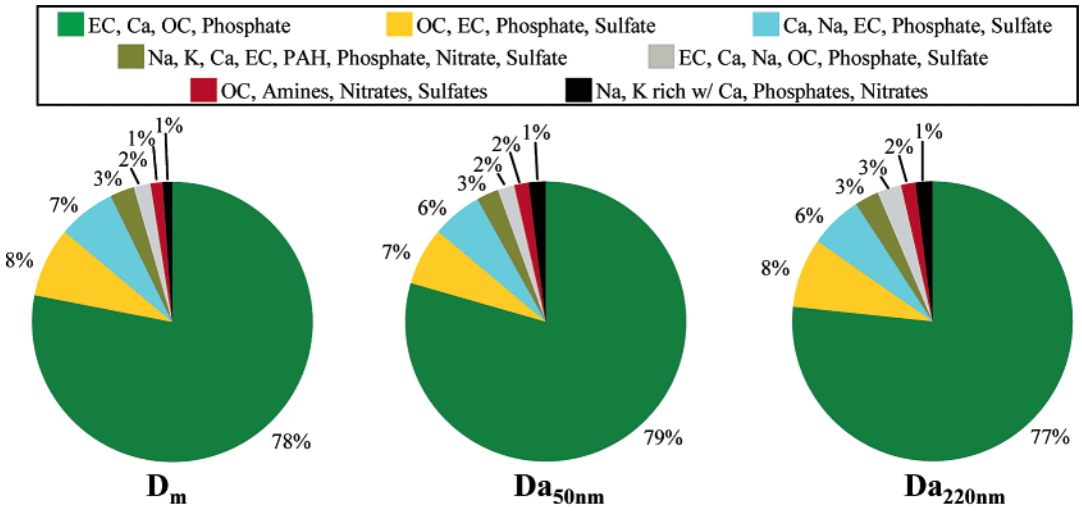

FIGURE 2. Statistical breakdown of the scaled particle classes observed from the HDDV exhaust. Particle statistics are shown for data scaled directly to SMPS data (D_m) and for SMPS data that were converted to D_a using shape factors and densities for diesel particles, as described in Park et al., with mobility diameters of 50 and 220 nm (D_{a50nm} and D_{a220nm}).

this class has a very similar composition to that of the third class, it differs by having much more intense EC ion intensities, as well as the presence of some OC. Despite these differences, this class does appear to be derived from the same process as the third class, and it may have just experienced slightly higher laser powers.

The sixth class, represented in Figure 1F (labeled OC, amines, nitrates, and sulfates in Figure 2), makes up 1% and appears to be from incomplete combustion of the diesel fuel. The negative ion peaks due to nitrate are an indication of incomplete combustion, and the presence of the sulfate species (with no presence of phosphate species) indicates that this is more likely from the combustion of fuel than from the lubricating oil. This source assignment is corroborated by the laboratory ATOFMS analysis of diesel fuel (*42*).

The final class, making up the remaining 1% of the total particles, is represented in Figure 1G (labeled Na, K rich w/Ca, phosphates, and nitrates in Figure 2). This class is very unique, as compared to the other classes, in that it is only composed of inorganic species. The species present in this class would indicate that the particles contained salts from the additives in the lubricating oil and fuel.

Analysis of Size-Segregated Chemical Composition for Each HDDV. To establish proper statistical representation of the particle classes, the UF-ATOFMS particle counts were scaled to particle counts detected with an SMPS. The same methods for scaling particle number concentration as described in Sodeman et al. and Robert et al. were used on the data in this study (*27*, *49*). The SMPS size bins were combined to ensure that there were enough UF-ATOFMS particle counts in each bin to provide reliable particle statistics. The rule set for scaling required each size bin to contain at least 10 particles detected by the UF-ATOFMS. Since UF-ATOFMS measures the particles' aerodynamic diameter (D_a) and this data was being scaled using an instrument (SMPS) that measures the particle mobility diameter (D_m), it was necessary to examine the effect of scaling to D_m without converting D_m to D_a. This was done using an equation for converting D_a to D_m as described in Van Gulijk et al. using the dynamic shape factors and particle densities as described in Park et al. (*44*, *50*). The shape factors reported in Park et al. are 1.11 and 2.21, and the particle densities used were 1.27 and 1.78 g/cm^3 for particles with mobility diameters of 50 and 200 nm, respectively. Figure 2 displays the results of this conversion for the percentages of the scaled classes. These results show that there is never more than a 1% deviation in the particle class contributions regardless of whether aerodynamic or mobility particles sizes are used. While D_m and D_a for diesel exhaust particles are not identical, it can be seen that only minor differences in the particle class statistics occur when scaling using the two different types of particle diameters. Thus, no modifications were made to the data to adjust for different chemical types for scaling since it was determined to be negligible for this study over this size range with the UF-ATOFMS.

Studies by Tobias et al. and Sakurai et al. investigated the chemical composition of particles as a function of size in HDDV engine emissions, but not at the single particle level, or using instruments with the ability to detect inorganic or refractory species (i.e., EC) (*18*, *20*). One of the unique measurement capabilities of ATOFMS or any single particle mass spectrometer that uses a laser for the desorption/ionization step is that OC, EC, and inorganic species can all be detected, and their associations within single particles can be measured in real time. This allows one to obtain size-resolved chemical composition information about the particle classes observed for each HDDV as shown in Figure 3. The UF-ATOFMS particle classes shown in Figure 3 are scaled to the SMPS number concentrations for combined size bins per gram of CO_2 for each HDDV on each test. The data in each plot have been multiplied by a factor (as indicated on each plot) to keep them all on the same scale. Data missing from a certain size bin indicate that there were not enough UF-ATOFMS particle counts for that particular bin to make scaling of that size bin statistically reliable.

As Figure 3 shows, the main particle type for generally all size bins and for each HDDV is the first particle class (EC, Ca, OC, and phosphate). This is particularly true for the smaller size bins, but as the particle size increases, the composition changes for some HDDVs. E55CRC-30 (Figure 3D,E) is an anomaly to this scenario, where the idle/creep cycle (Figure 3D) is dominated by the second particle class (OC, EC, phosphate, and sulfate) for all size bins and still contains a significant amount of particles in this class even for the five-cycle test (Figure 3E). Since the HDDVs E55CRC-27, -28, and -30 (Figure 3A−D) have enough counts to show scaled data out to 294 nm, trends in particle composition can be examined as the size increases. The larger size bins show that some of the more minor classes (especially the OC-containing classes) begin to become more prevalent as the particle size increases. This is an indication of semivolatile organic vapors condensing onto HDDV exhaust particle EC cores to create larger particles with contributions from organic carbon species (*51*). For each HDDV, from 50 to 178

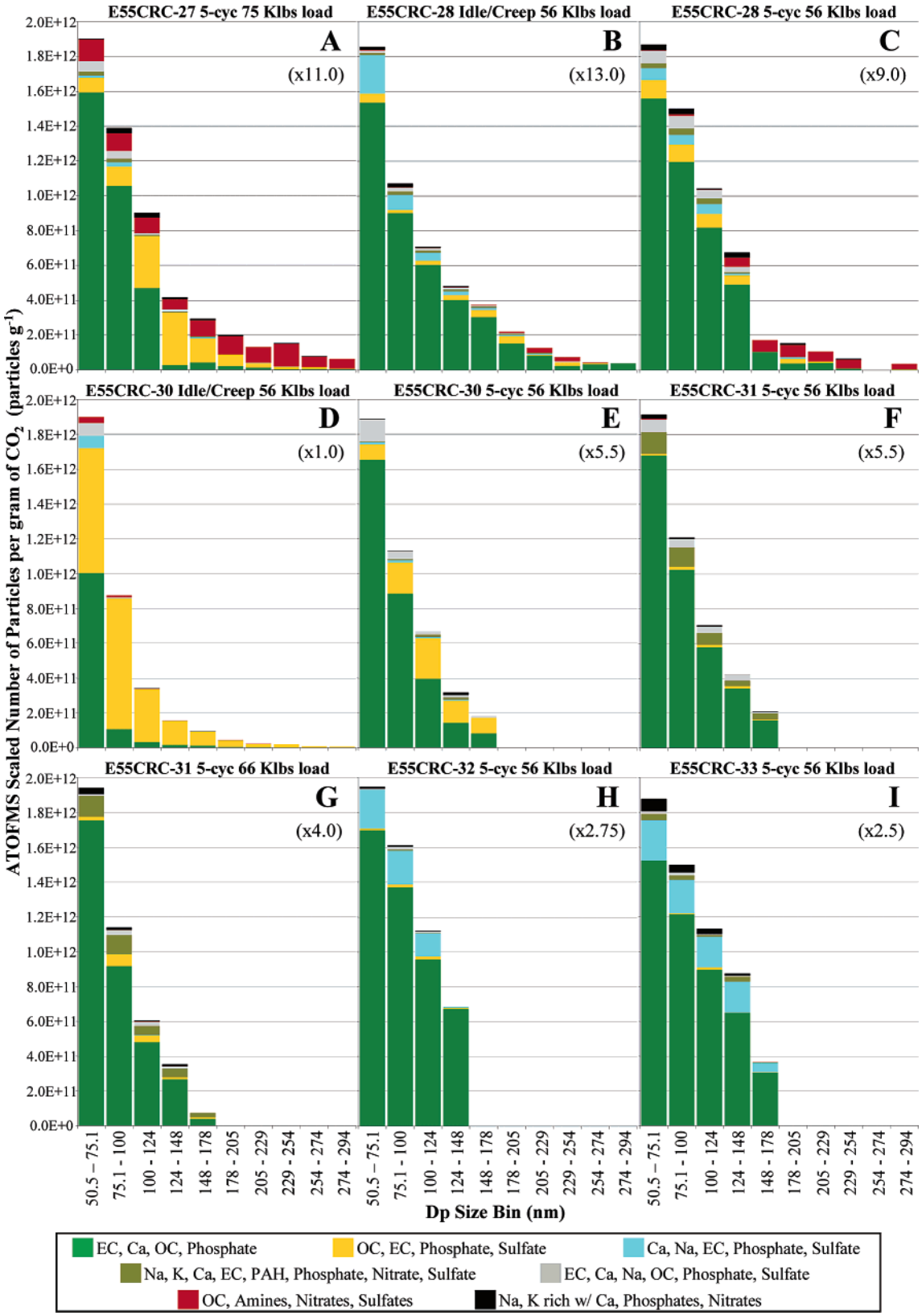

FIGURE 3. (A–I) UF-ATOFMS size-segregated chemical composition of particles observed for each HDDV for each driving test scaled number to SMPS per gram of CO_2. Size bins are created from SMPS data, where bins were combined to provide 20–25 nm size bins. The simulated on-axle weight load is provided for each HDDV.

nm, the overall particle class breakdown per size bin seems to be relatively constant (excluding E55CRC-27 and -30). In addition, each of the HDDVs tested was found to emit the same particle types. The difference between the HDDVs is the proportions of each particle type emitted.

Another feature to note about Figure 3 concerns the number concentration as a function of size for each HDDV. The scale is set by E55CRC-30 (Figure 3D) during the idle/creep cycle, where particle concentrations peaked in the 50–75 nm size bin. The number concentrations fall quite

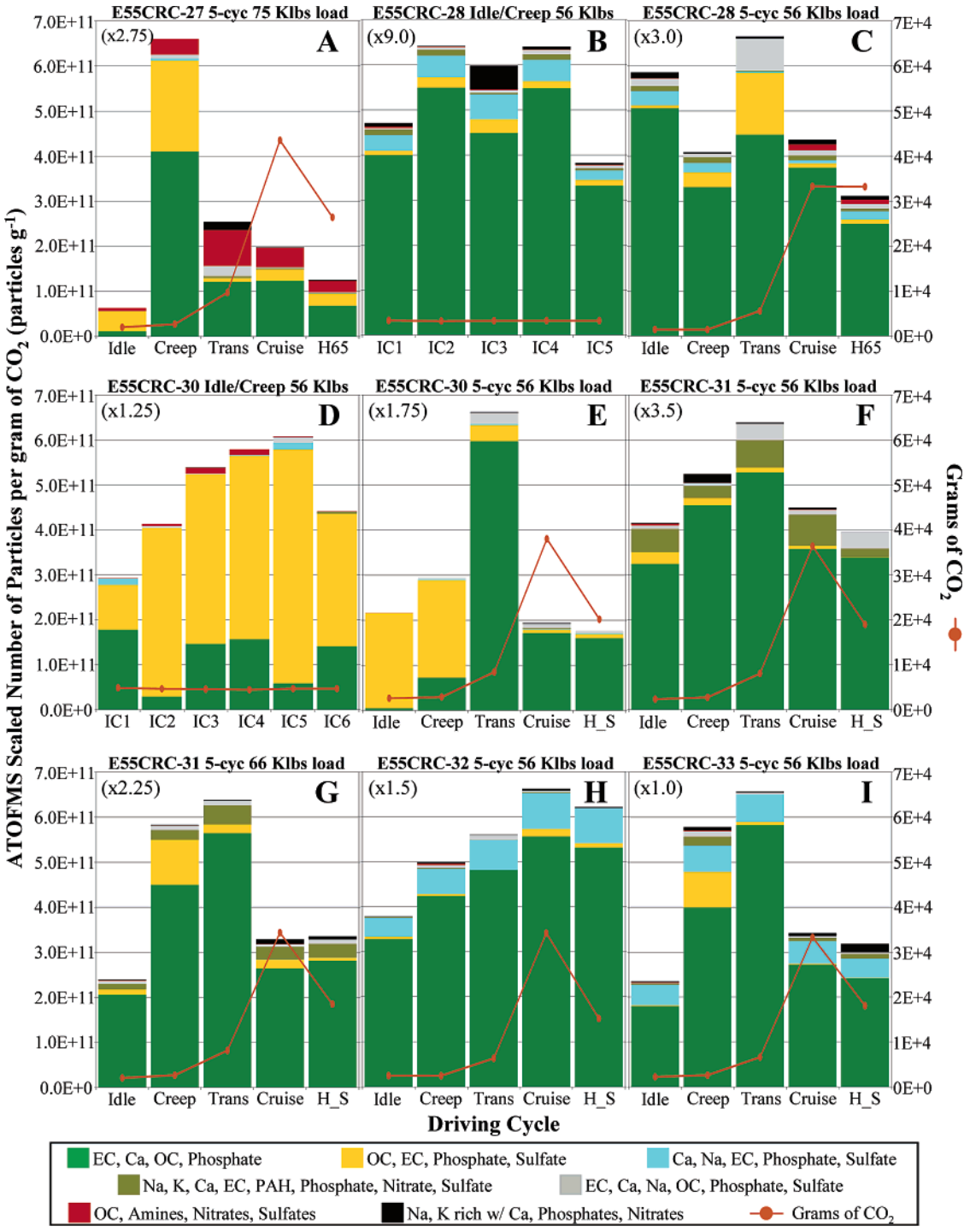

FIGURE 4. (A−I) UF-ATOFMS particle class scaled number to SMPS per gram of CO_2 for each HDDV on each test cycle. Measured CO_2 concentrations for each cycle are included for each HDDV. The simulated on-axle weight load is provided for each HDDV. Note: the high-speed HHDDT65 cycle is denoted as H65, and the modified high-speed HDDT_S cycle is denoted as H_S.

dramatically with this particular HDDV as the particle size increases, as expected for an idle/creep cycle. The size-distribution of the idle/creep cycle for E55CRC-28 (Figure 3B) does not show this type of trend though, which is particularly interesting since they are of the same make/model and year (and E55CRC-28 has a higher engine mileage). Another interesting note is in regards to E55CRC-31, which ran the five-cycle test at simulated on-axle weight loads of 56,000 and 66,000 lbs (Figure 3F,G). The particulate emissions for the 66,000 lbs test were a little over 1.5 times more per size bin than for the 56,000 lbs test. However, it is noticeable that for each size bin, the relative particle composition remains fairly constant between the two loads. Another trend that can be noted from all the HDDVs (excluding E55CRC-30) is that the particle number concentrations over all size bins (50−294 nm) tend to increase with older HDDV models.

Particle Composition as a Function of Driving Cycle and HDDV. It is expected that different HDDVs will have somewhat different particle compositions in their exhaust. Differences in fuel, oil, engine technology, and engine wear play a role in these particle composition variations. Figure 4(A−I) shows the UF-ATOFMS particle classes scaled to the SMPS number concentrations per gram of CO_2 for each HDDV on each test cycle. The measured CO_2 concentrations for

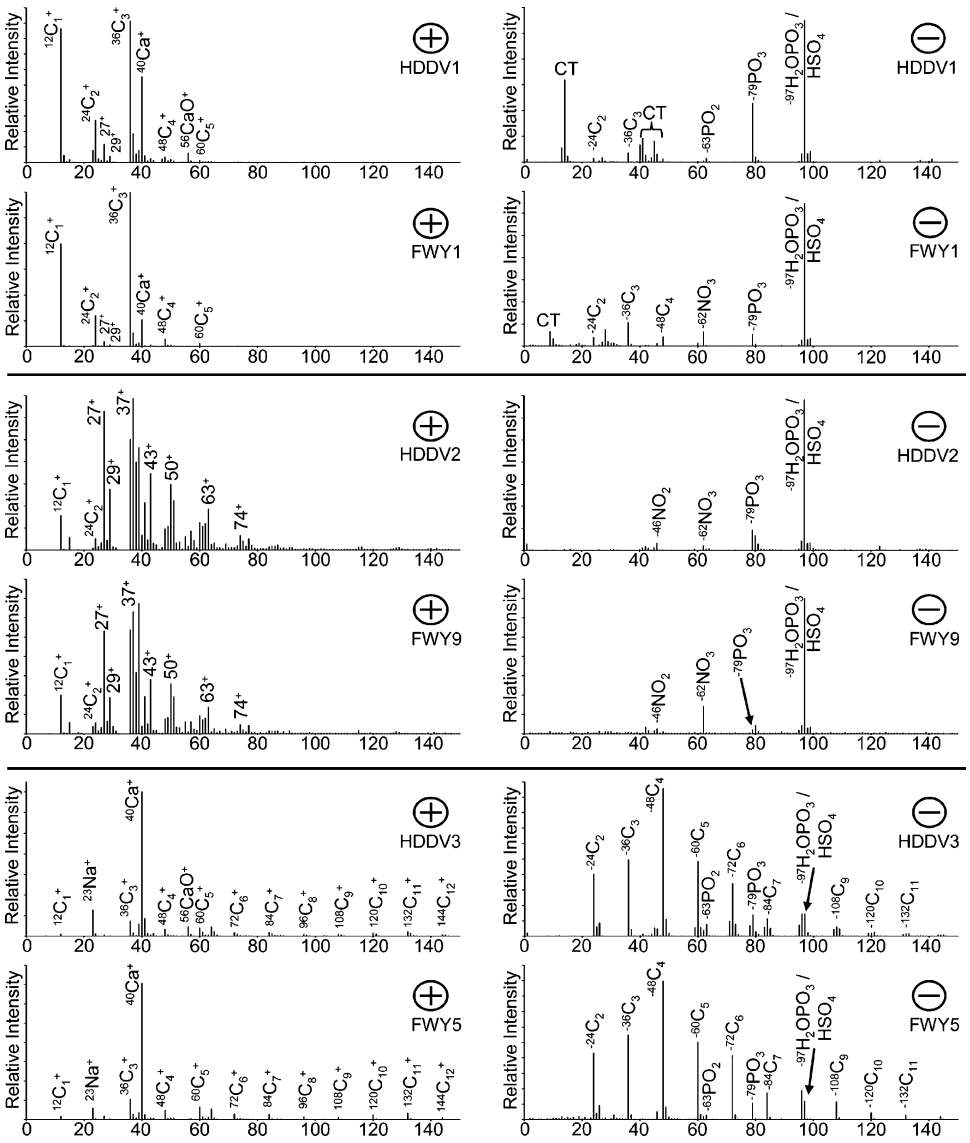

FIGURE 5. Comparison of the top three HDDV particle classes with those observed of the same type in an ambient freeway study with the UF-ATOFMS. HDDV classes are labeled as HDDV# (±), and the classes from the freeway study are labeled as FWY# (±). The # for HDDV and FWY refers to the cluster result as classified with ART-2a. The freeway study was classified using the same ART-2a parameters as the HDDV study. Similar classes are stacked together.

each cycle are also included in this plot to show the trend of CO_2 emission. Since UF-ATOFMS is unable to detect particles below 50 nm, the number concentration trends per cycle for these plots in Figure 4 will follow the trend for each cycle within the dashed lines shown in the Supporting Information, Figure S2. Also, the data from each plot in Figure 4 have been multiplied by a factor (indicated on each plot) to keep them all on the same scale.

As shown, the specific driving conditions can produce different types of particles. This is more clearly shown for the minor classes, as they can occur in relatively high abundance for just one cycle for a particular HDDV. E55CRC-27 and -30 show the most variation due to a major contribution from OC particles. These plots (as well as those in the previous figure) show that not all HDDVs produce the same abundance of particle types. This is even true for E55CRC-28 and -30 (Figure 4B−E), which are the same make/model and year but emit different amounts of the same particle types on the same driving cycles.

Since there were only six HDDVs tested in this study, it is difficult to make generalizations for all HDDVs and driving cycles based on these results. One trend that remains consistent is the presence of the top particle class (EC, Ca, OC, and phosphate) for all HDDVs tested. While this may not have always been the dominant class for every cycle and size bin, it was consistently emitted from each HDDV tested and may therefore be useful for ambient apportionment purposes as discussed later. In general, only one HDDV (E55CRC-30) emitted high amounts of OC particles both in number concentration measured with the UF-ATOFMS and mass concentration measured on filters by the Kleeman group (*27*).

Composition and Reproducibility Over a Larger Size Range. A previous study on HDDV particle emissions was conducted with a standard inlet ATOFMS on the same dynamometer system in Riverside, CA in 2001 (*31*). While the ATOFMS instrument used for the earlier HDDV study was tuned to characterize particles down to 100 nm, it had a much lower transmission efficiency for smaller particles than the UF-ATOFMS (*17*). The size overlap allows for comparison of particle types detected by two different ATOFMS instruments; however, it is important to note that the UF-ATOFMS will have better compositional statistics at smaller sizes based on its higher transmission efficiency.

As with the particle classes observed in this study, the top particle classes from the 2001 study were dominated by particles attributed to EC and diesel lubricating oil. With the standard inlet ATOFMS, as particle size becomes smaller, the classes match well with those obtained with UF-ATOFMS. The top particle class seen with both instruments in the 100−300 nm size range is the EC, Ca, OC, and phosphate type. When the ion intensities between the two weight matrices are plotted against each other, an R^2 value of 0.95 is obtained for the top ART-2a cluster of this class between the two studies. The other main class seen with the standard inlet ATOFMS matches the third most abundant class (Ca, Na, EC, phosphate, and sulfate) seen with the UF-ATOFMS and also shows a strong correlation ($R^2 = 0.95$). The sixth and seventh classes are also seen in this overlapping size range between the two studies with R^2 correlations of 0.88 and 0.87. The other particle types detected with the UF-ATOFMS (the second, fourth, and fifth classes listed in this paper) were also observed in the previous study with the standard inlet instrument; however, the particle counts for these types were not sufficient to be included as their own classes and were grouped into a minor classes category. Because of the overall higher transmission of particles in this size range in the UF-ATOFMS, there is a better statistical representation of the classes containing fewer particles that allows them to be classified into their own distinct chemical category with the UF-ATOFMS.

The previous evaluation focuses on the comparison of particle signatures only for particles of the same size. When comparing the composition of all particle sizes, both instruments detected similar OC and EC particle types; however, the ordering of abundance changes. Such classes include the top class, the third class, the sixth class, and the seventh class with R^2 correlations of 0.89, 0.81, 0.78, and 0.76, respectively. These correlations were higher than expected given that the two instruments detect the majority of their particles in different size ranges. In general, for particles classified as the same type in the two studies, the larger particles detected with the standard inlet ATOFMS show more aged/complex spectra than those detected with the UF-ATOFMS for the same classified particle type in the smaller sizes. Specifically, higher mass EC ion peaks and more negative ion peaks were detected from particles with the standard inlet ATOFMS than with the UF-ATOFMS, which is reflected in the lower R^2 correlations for the EC types. This could be reflective of larger soot agglomerates at larger sizes leading to more extensive EC carbon cluster ion patterns (*44*, *52*). The fact that the chemistry and particle types do not change significantly as the particle size increases, only the intensities increase, suggests that particle growth via agglomeration is the main growth mechanism for these particles types. In the atmosphere, since particle composition can be affected by gases and particles from different sources with different compositions, one might expect larger ambient particles to have distinctly different compositions than smaller particles (*53*). In fact, this is indeed what is observed in ambient ATOFMS studies. For a further description of the unique larger particles detected with the standard inlet instrument, see Shields et al. (*31*).

Prospects for Apportionment. One of the key goals of this study involved obtaining source signatures for HDDVs that can be used for source apportionment of ambient particles. A question exists as to whether mass spectral signatures from different sources obtained from laboratory and dynamometer experiments can be detected during ambient studies and used for source apportionment. Part of this comes from concern that the particle sizes and compositions sampled from the tailpipe of HDDVs (through the dilution and residence systems) do not properly mimic the dilution and aging that occurs on these particles in real on-road driving (*54*, *55*). Certain sources, such as sea salt, dust, light duty gasoline powered vehicles, biomass burning, coal combustion, meat cooking, and fireworks have proven to be readily distinguishable in ATOFMS ambient measurements by using source signatures to apportion them (*49*, *56*−*62*). A far bigger challenge involves distinguishing exhaust particles from gasoline and diesel powered vehicles in an ambient environment. Comparing the source signatures for gasoline powered light duty vehicles (LDV) obtained in Sodeman et al. (*49*) versus those obtained for HDDV with UF-ATOFMS has shown that the particles from these sources are distinguishable from one another and will be described in further detail in a future manuscript (*63*). In short, some features that can be used to distinguish HDDV from LDV are more intense peaks for calcium and phosphate, and the intensity of the peak at $^{36}C_3^+$ is greater than that of $^{12}C_1^+$ in EC particles emitted from HDDV particles. While there is some similarity between LDV and HDDV exhaust particle types, they are mathematically discernible with ART-2a.

Figure 5 displays the top three ART-2a clusters/classes from this HDDV characterization study as compared to the first, fifth, and ninth most abundant classes observed with the UF-ATOFMS sampling alongside a freeway (in the 50−300 nm size range). When ion peak intensities for each m/z of the weight matrices (representative spectra) in the classes being compared are plotted against one another, very close correlations exist with R^2 values of 0.89, 0.95, and 0.97 for HDV1-FWY1, HDV2-FWY9, and HDV3-FWY5, respectively. As shown here, the dynamometer classes are detected in ambient air with almost identical signatures at the single particle level, thus showing promise that dynamometer signatures can be used for future ambient source apportionment. A more detailed analysis of the ambient freeway study concerning the ability to match fresh dynamometer emissions with fresh ambient roadside emissions will be forthcoming. The issue of ambient aging and how this affects apportionment will also be addressed in future papers.

Acknowledgments

The authors thank Nigel Clark and the personnel at the WVU portable HDDV dynamometer facility in Riverside, CA (including Tom Long, Curt Leasor, Chris Rowe, and Adam Leach) for their assistance in vehicle testing providing gas phase data. We also sincerely thank Michael Kleeman, Michael Robert, and Chris Jakober for operating the secondary dilution and residence chamber. Last, we thank William Vance from the California Air Resources Board (CARB) for all the help he provided with the WVU data. Funding for this project was supplied by CARB Contract 00-331.

Supporting Information Available

More detailed descriptions of the experimental and particle type description sections of this paper; brief description on size-distribution analysis; driving time and dilution conditions for each cycle driven for each HDDV (Table S1); diagram of the sampling system derived from Robert et al. (*27*) (Figure S1); and average size-distributions (from SMPS) for all HDDVs during each of the five-cycle tests (Figure S2). This material is available free of charge via the Internet at http://pubs.acs.org.

Literature Cited

(1) Kittelson, D. B. Engines and Nanoparticles—a Review. *J. Aerosol Sci.* **1998**, *29*, 575−588.

(2) Reed, M. D.; Gigliotti, A. P.; McDonald, J. D.; Seagrave, J. C.; Seilkop, S. K.; Mauderly, J. L. Health Effects of Subchronic Exposure to Environmental Levels of Diesel Exhaust. *Inhalation Toxicol.* **2004**, *16*, 177−193.

(3) Zhao, H. W.; Barger, M. W.; Ma, J. K. H.; Castranova, V.; Ma, J. Y. C. Effects of exposure to diesel exhaust particles (DEP) on

pulmonary metabolic activation of mutagenic agents. *Mutat. Res.* **2004**, *564*, 103−113.
(4) Dybdahl, M.; Risom, L.; Bornholdt, J.; Autrup, H.; Loft, S.; Wallin, H. Inflammatory and genotoxic effects of diesel particles in vitro and in vivo. *Mutat. Res.* **2004**, *562*, 119−131.
(5) Pourazar, J.; Frew, A. J.; Blomberg, A.; Helleday, R.; Kelly, F. J.; Wilson, S.; Sandstrom, T. Diesel exhaust exposure enhances the expression of IL-13 in the bronchial epithelium of healthy subjects. *Respir. Med.* **2004**, *98*, 821−825.
(6) Shi, J. P.; Mark, D.; Harrison, R. M. Characterization of particles from a current technology heavy duty diesel engine. *Environ. Sci. Technol.* **2000**, *34*, 748−755.
(7) Schauer, J. J.; Kleeman, M. J.; Cass, G. R.; Simoneit, B. R. T. Measurement of emissions from air pollution sources. 2. C-1 through C-30 organic compounds from medium duty diesel trucks. *Environ. Sci. Technol.* **1999**, *33*, 1578−1587.
(8) Moosmuller, H.; Arnott, W. P.; Rogers, C. F.; Bowen, J. L.; Gillies, J. A.; Pierson, W. R.; Collins, J. F.; Durbin, T. D.; Norbeck, J. M. Time-resolved characterization of diesel particulate emissions. 1. Instruments for particle mass measurements. *Environ. Sci. Technol.* **2001**, *35*, 781−787.
(9) Reilly, P. T. A.; Gieray, R. A.; Whitten, W. B.; Ramsey, J. M. Real-Time Characterization of the Organic Composition and Size of Individual Diesel Engine Smoke Particles. *Environ. Sci. Technol.* **1998**, *32*, 2672−2679.
(10) Lehmann, U.; Mohr, M.; Schweizer, T.; Rutter, J. Number size distribution of particulate emissions of heavy duty engines in real world test cycles. *Atmos. Environ.* **2003**, *37*, 5247−5259.
(11) Sakurai, H.; Park, K.; McMurry, P. H.; Zarling, D. D.; Kittelson, D. B.; Ziemann, P. J. Size-Dependent Mixing Characteristics of Volatile and Nonvolatile Components in Diesel Exhaust Aerosols. *Environ. Sci. Technol.* **2003**, *37*, 5487−5495.
(12) Khalek, I. A.; Spears, M.; Charmley, W. Particle size distribution from a heavy duty diesel engine: Steady-state and transient emission measurement using two dilution systems and two fuels. *Soc. Automot. Eng., [Spec. Publ.] SP* **2003**, *1755*, 1−11.
(13) Lyyranen, J.; Jokiniemi, J.; Kauppinen, E. I.; Joutsensaari, J. Aerosol characterization in medium-speed diesel engines operating with heavy fuel oils. *J. Aerosol Sci.* **1999**, *30*, 771−784.
(14) Virtanen, A. K. K.; Ristimaeki, J. M.; Vaaraslahti, K. M.; Keskinen, J. Effect of Engine Load on Diesel Soot Particles. *Environ. Sci. Technol.* **2004**, *38*, 2551−2556.
(15) Kwon, S.-B.; Lee, K. W.; Saito, K.; Shinozaki, O.; Seto, T. Size-Dependent Volatility of Diesel Nanoparticles: Chassis Dynamometer Experiments. *Environ. Sci. Technol.* **2003**, *37*, 1794−1802.
(16) Yanowitz, J.; Graboski, M. S.; Ryan, L. B. A.; Alleman, T. L.; McCormick, R. L. Chassis dynamometer study of emissions from 21 in-use heavy duty diesel vehicles. *Environ. Sci. Technol.* **1999**, *33*, 209−216.
(17) Su, Y.; Sipin, M. F.; Furutani, H.; Prather, K. A. Development and Characterization of an Aerosol Time-of-Flight Mass Spectrometer with Increased Detection Efficiency. *Anal. Chem.* **2004**, *76*, 712−719.
(18) Tobias, H. J.; Beving, D. E.; Ziemann, P. J.; Sakurai, H.; Zuk, M.; McMurry, P. H.; Zarling, D.; Waytulonis, R.; Kittelson, D. B. Chemical Analysis of Diesel Engine Nanoparticles Using a Nano-DMA/Thermal Desorption Particle Beam Mass Spectrometer. *Environ. Sci. Technol.* **2001**, *35*, 2233−2243.
(19) Tobias, H. J.; Kooiman, P. M.; Docherty, K. S.; Ziemann, P. J. Real-time chemical analysis of organic aerosols using a thermal desorption particle beam mass spectrometer. *Aerosol Sci. Technol.* **2000**, *33*, 170−190.
(20) Sakurai, H.; Tobias, H. J.; Park, K.; Zarling, D.; Docherty, K. S.; Kittelson, D. B.; McMurry, P. H.; Ziemann, P. J. On-line measurements of diesel nanoparticle composition and volatility. *Atmos. Environ.* **2003**, *37*, 1199−1210.
(21) Jayne, J. T.; Leard, D. C.; Zhang, X.; Davidovits, P.; Smith, K. A.; Kolb, C. E.; Worsnop, D. R. Development of an aerosol mass spectrometer for size and composition analysis of submicron particles. *Aerosol Sci. Technol.* **2000**, *33*, 49−70.
(22) Canagaratna, M. R.; Jayne, J. T.; Ghertner, D. A.; Herndon, S.; Shi, Q.; Jimenez, J. L.; Silva, P. J.; Williams, P.; Lanni, T.; Drewnick, F.; Demerjian, K. L.; Kolb, C. E.; Worsnop, D. R. Chase studies of particulate emissions from in-use New York City vehicles. *Aerosol Sci. Technol.* **2004**, *38*, 555−573.
(23) Watson, J. G.; Chow, J. C.; Lowenthal, D. H.; Pritchett, L. C.; Frazier, C. A. Differences in the carbon composition of source profiles for diesel- and gasoline-powdered vehicles. *Atmos. Environ.* **1994**, *28*, 2493−2505.
(24) Suess, D. T.; Prather, K. A. Reproducibility of single particle chemical composition during a heavy duty diesel truck dynamometer study. *Aerosol Sci. Technol.* **2002**, *36*, 1139−1141.
(25) Clark, N. N.; Gautam, M.; Bata, R. M.; Wang, W.-G.; Loth, J. L.; Palmer, G. M.; Lyons, D. W. Technical Report: Design and operation of a new transportable laboratory for emissions testing of heavy duty trucks and busses. *Int. J. Vehicle Des* **1995**, *2*, 308−322.
(26) Bata, R.; Clark, N.; Gautam, M.; Howell, A.; Long, T.; Loth, J.; Lyons, D.; Palmer, G.; Smith, J.; Wang, W. A Transportable Heavy Duty Engine Testing Laboratory. *SAE Trans.* **1991**, *100*, 433−440.
(27) Robert, M. A.; Jakober, C. A.; Kleeman, M. J. Size and composition distributions of particulate matter emissions. 2. Heavy duty diesel vehicles. **2006**, submitted for publication.
(28) Song, X. H.; Hopke, P. K.; Fergenson, D. P.; Prather, K. A. Classification of single particles analyzed by ATOFMS using an artificial neural network, ART-2A.. *Anal. Chem.* **1999**, *71*(4), 860−865.
(29) Hopke, P. K.; Song, X. H. Classification of Single Particles by Neural Networks Based on the Computer-Controlled Scanning Electron Microscopy Data. *Anal. Chim. Acta.* **1997**, *348*, 375−388.
(30) Xie, Y.; Hopke, P. K.; Wienke, D. Airborne Particle Classification with a Combination of Chemical Composition and Shape Index Utilizing an Adaptive Resonance Artificial Neural Network. *Environ. Sci. Technol.* **1994**, *28*, 1921−1928.
(31) Shields, L. G.; Suess, D. T.; Guazzotti, S. A.; Prather, K. A. Determination of single particle mass spectral signatures from heavy duty vehicle emissions in the 0.1−3 ìm size range. **2006**, manuscript in preparation.
(32) Burtscher, H.; Kunzel, S.; Huglin, C. Characterization of Particles in Combustion Engine Exhaust. *J. Aerosol Sci.* **1998**, *29*, 389−396.
(33) Gautam, M.; Chitoor, K.; Durbha, M.; Summers, J. C. Effect of diesel soot contaminated oil on engine wear—investigation of novel oil formulations. *Tribol. Intl.* **1999**, *32*, 687−699.
(34) Rudnick, L. R. *Lubricant additives: chemistry and applications*; Marcel Dekker: New York, 2003.
(35) Harrison, R. M.; Tilling, R.; Romero, M. S. C.; Harrad, S.; Jarvis, K. A study of trace metals and polycyclic aromatic hydrocarbons in the roadside environment. *Atmos. Environ.* **2003**, *37*, 2391−2402.
(36) Vilhunen, J. K.; Von Bohlen, A.; Schmeling, M.; Rantanen, L.; Mikkonen, S.; Klockenkamper, R.; Klockow, D. Trace element determination in diesel particulates by total-reflection X-ray fluorescence analysis. *Mikrochim. Acta* **1999**, *131*, 219−223.
(37) Jung, H.; Kittelson, D. B.; Zachariah, M. R. The influence of engine lubricating oil on diesel nanoparticle emissions and kinetics of oxidation. *Soc. Automot. Eng., [Spec. Publ.] SP* **2003**, *1802*, 217−226.
(38) Lyyranen, J.; Jokiniemi, J.; Kauppinen, E. I.; Joutsensaari, J. Aerosol characterization in medium-speed diesel engines operating with heavy fuel oils. *J. Aerosol Sci.* **1999**, *30*, 771−784.
(39) Okada, S.; Kweon, C.-B.; Stetter, J. C.; Foster, D. E.; Shafer, M. M.; Christensen, C. G.; Schauer, J. J.; Schmidt, A. M.; Silverberg, A. M.; Gross, D. S. Measurement of trace metal composition in diesel engine particulate and its potential for determining oil consumption: ICPMS (inductively coupled plasma mass spectrometer) and ATOFMS (aerosol time-of-flight mass spectrometer) measurements. *Soc. Automot. Eng., [Spec. Publ.] SP* **2003**, *1737*, 59−72.
(40) Lowenthal, D. H.; Zielinska, B.; Chow, J. C.; Watson, J. G.; Gautam, M.; Ferguson, D. H.; Neuroth, G. R.; Stevens, K. D. Characterization of heavy duty diesel vehicle emissions; *Atmos. Environ.* **1994**, *28*, 731−743.
(41) Kleeman, M. J.; Schauer, J. J.; Cass, G. R. Size and Composition Distribution of Fine Particulate Matter Emitted from Motor Vehicles. *Environ. Sci. Technol.* **2000**, *34*, 1132−1142.
(42) Spencer, M. T.; Shields, L. G.; Toner, S. M.; Sodeman, D. A.; Suess, D. T.; Prather, K. A. Atomization of gasoline and diesel fuel and oil. **2006**, accepted for publication.
(43) Arens, F.; Gutzwiller, L.; Baltensperger, U.; Gaeggeler, H. W.; Ammann, M. Heterogeneous Reaction of NO_2 on Diesel Soot Particles. *Environ. Sci. Technol.* **2001**, *35*, 2191−2199.
(44) Van Gulijk, C.; Marijnissen, J. C. M.; Makkee, M.; Moulijn, J. A.; Schmidt-Ott, A. Measuring diesel soot with a scanning mobility particle sizer and an electrical low-pressure impactor: performance assessment with a model for fractal-like agglomerates. *J. Aerosol Sci.* **2004**, *35*, 633−655.
(45) Walker, A. P. Controlling particulate emissions from diesel vehicles. *Top. Catal.* **2004**, *28*, 165−170.
(46) Wenzel, R. J.; Prather, K. A. Improvements in ion signal reproducibility obtained using a homogeneous laser beam for

on-line laser desorption/ionization of single particles. *Rapid Commun. Mass Spectrom.* **2004**, *18*, 1525−1533.
(47) Zielinska, B.; Sagebiel, J.; Arnott, W. P.; Rogers, C. F.; Kelly, K. E.; Wagner, D. A.; Lighty, J. S.; Sarofim, A. F.; Palmer, G. Phase and Size Distribution of Polycyclic Aromatic Hydrocarbons in Diesel and Gasoline Vehicle Emissions. *Environ. Sci. Technol.* **2004**, *38*, 2557−2567.
(48) Rhead, M. M.; Hardy, S. A. The sources of polycyclic aromatic compounds in diesel engine emissions. *Fuel* **2003**, *82*, 385−393.
(49) Sodeman, D. A.; Toner, S. M.; Prather, K. A. Determination of Single Particle Mass Spectral Signatures from Light Duty Vehicle Emissions. *Environ. Sci. Technol.* **2005**, *39*, 4569−4580.
(50) Park, K.; Kittelson, D. B.; McMurry, P. H. Structural properties of diesel exhaust particles measured by transmission electron microscopy (TEM): Relationships to particle mass and mobility. *Aerosol Sci. Technol.* **2004**, *38*, 881−889.
(51) Spencer, M. T.; Prather, K. A. Using ATOFMS to estimate the fractions of EC and OC in soot particles. *Anal. Chem*. **2006**, accepted for publication.
(52) Park, K.; Kittelson, D. B.; Zachariah, M. R.; McMurry, P. H. Measurement of Inherent Material Density of Nanoparticle Agglomerates. *J. Nanopart. Res.* **2004**, *6*, 267−272.
(53) Jacobson, M. Z.; Seinfeld, J. H. Evolution of nanoparticle size and mixing state near the point of emission. *Atmos. Environ.* **2004**, *38*, 1839−1850.
(54) Kawai, T.; Goto, Y.; Odaka, M. Influence of dilution process on engine exhaust nanoparticles. *Soc. Automot. Eng., [Spec. Publ.] SP* **2004**, *1862*, 113−119.
(55) Graskow, B. R.; Ahmadi, M. R.; Morris, J. E.; Kittelson, D. B. Influence of fuel additives and dilution conditions on the formation and emission of exhaust particulate matter from a direct injection spark ignition engine. *Soc. Automot. Eng., [Spec. Publ.] SP* **2000**, *1551*, 261−271.
(56) Gard, E. E.; Kleeman, M. J.; Gross, D. S.; Hughes, L. S.; Allen, J. O.; Morrical, B. D.; Fergenson, D. P.; Dienes, T.; Galli, M. E.; Johnson, R. J.; Cass, G. R.; Prather, K. A. Direct observation of heterogeneous chemistry in the atmosphere. *Science* **1998**, *279*, 1184−1187.
(57) Silva, P. J.; Carlin, R. A.; Prather, K. A. Single particle analysis of suspended soil dust from Southern California. *Atmos. Environ.* **2000**, *34*, 1811−1820.
(58) Silva, P. J.; Liu, D.-Y.; Noble, C. A.; Prather, K. A. Size and Chemical Characterization of Individual Particles Resulting from Biomass Burning of Local Southern California Species. *Environ. Sci. Technol.* **1999**, *33*, 3068−3076.
(59) Liu, D.-Y.; Rutherford, D.; Kinsey, M.; Prather, K. A. Real-Time Monitoring of Pyrotechnically Derived Aerosol Particles in the Troposphere. *Anal. Chem*. **1997**, *69*, 1808−1814.
(60) Suess, D. T. Single Particle Mass Spectrometry Combustion Source Characterization and Atmospheric Apportionment of Vehicular, Coal, and Biofuel Exhaust Emissions. Ph.D. Dissertation, University of California, Riverside, 2002; p 377.
(61) Liu, D.-Y.; Wenzel, R. J.; Prather, K. A. Aerosol time-of-flight mass spectrometry during the Atlanta Supersite Experiment: 1. Measurements. *J. Geophys. Res.* **2003**, *108*, SOS 14/11 to SOS 14/16.
(62) Guazzotti, S. A.; Suess, D. T.; Coffee, K. R.; Quinn, P. K.; Bates, T. S.; Wisthaler, A.; Hansel, A.; Ball, W. P.; Dickerson, R. R.; Neususs, C.; Crutzen, P. J.; Prather, K. A. Characterization of carbonaceous aerosols outflow from India and Arabia: biomass/biofuel burning and fossil fuel combustion. *J. Geophys. Res.* **2003**, *108*, ACL13/11 to ACL13/14.
(63) Toner, S. M.; Shields, L. G.; Sodeman, D. A.; Prather, K. A. Using Mass Spectral Source Signatures to Apportion Exhaust Particles from Gasoline and Diesel Powered Vehicles in a Freeway Study using UF-ATOFMS. **2006**, manuscript in preparation.

Received for review July 25, 2005. Revised manuscript received February 13, 2006. Accepted April 14, 2006.

ES051455X